Scanning Microscopy

Volume 5 | Number 2 Article 21

3-14-1991

# Ultrastructure of Coronary Arterial Endothelium in Atherosclerotic Swine Suggests Lipid Retro-Endocytosis

Keith A. Robinson
*Western Carolina University*

Robert P. Apkarian
*Emory University*

Scanning Microscopy, Vol. 5, No. 2, 1991 (Pages 533-539) 0891-7035/91$3.00+.00
Scanning Microscopy International, Chicago (AMF O'Hare), IL 60666 USA

# ULTRASTRUCTURE OF CORONARY ARTERIAL ENDOTHELIUM IN ATHEROSCLEROTIC SWINE SUGGESTS LIPID RETRO-ENDOCYTOSIS

Keith A. Robinson* and Robert P. Apkarian[1]

Western Carolina University,
Cullowhee, North Carolina, 28723
[1]Yerkes Regional Primate Research Center, Emory University,
Atlanta, Georgia, 30322

(Received for publication October 25, 1990, and in revised form March 14, 1991)

## Abstract

During experimental atherosclerosis, arterial endothelial cells show characteristic ultrastructural changes including the appearance of increased numbers of plasmalemmal and cytoplasmic vesicles. These structures have been shown by tracer studies to participate in the transcellular transport of low-density lipoprotein cholesterol and $\beta$-very-low-density lipoprotein cholesterol from the arterial lumen into the abluminal extracellular matrix. Although this probably represents the major lipid transport pathway, other forms of transport may exist. We document the presence of apparent lipid structures averaging approximately 300 nm in diameter at or near the luminal surface of coronary arterial endothelium of atherosclerotic miniature swine. The structures exhibited a particulate nature with subunits of a heterogenous size distribution. The appearance of the endothelial plasmalemma adjacent and subjacent to these structures suggests exocytosis. We hypothesize that this previously unreported morphology may represent an in vivo structural correlate for the lipoprotein retro-endocytosis pathway which has been recently identified using biochemical methods in smooth muscle cells and fibroblasts in vitro.

**Key words**: atherosclerosis, endothelium, electron microscopy, lipid, lipoprotein, cholesterol, endothelial cells, ultrastructure, retro-endocytosis.

***Address for correspondence**:
Keith A. Robinson
Dept. HPER, Reid Gymnasium
Western Carolina University
Cullowhee, NC 28723

Phone: (704) 227 7332

## Introduction

Certain structural and ultrastructural changes in arterial endothelial cells (EC) which accompany diet- and injury-induced atherosclerosis have been described for various animal species (5, 6, 10-13), and recently similar changes have been observed using scanning and transmission electron microscopy (SEM & TEM) of atherosclerotic human tissue (4, 7). Vasile, et al. (13) demonstrated that a low affinity, nonsaturable plasmalemmal-cytoplasmic vesicle mechanism operates to transport low-density lipoprotein cholesterol across aortic endothelium in rabbits fed excess fat and cholesterol. Vasile et al. (12) later found the same or a similar pathway exists for $\beta$-very-low-density lipoprotein cholesterol as well. These findings supported earlier purely morphological observations of increased numbers of luminal and abluminal plasmalemmal vesicles and EC channels (5, 6, 11) which had suggested that these structures might be responsible for endocytic and transcellular lipid transport.

Simionescu et al. (10) described the appearance of cholesterol-rich liposomes in the subendothelial extracellular matrix early in the onset of atherosclerosis in rabbits, after initiation of lipid supplementation but before the appearance of foam cell lesions. Similar structures, among others, have been observed in atherosclerotic plaques from human aortas. Bocan, et al. (4) examined the core and peripheral regions of fibrolipid lesions using TEM with osmium-thiocarbohydrazide-osmium staining, finding lipid droplets and vesicles as well as cholesterol clefts, and concluded that lipid deposition in the extracellular matrix is not a result of cell necrosis but occurs early in lesion development (4). Thus, the enhanced uptake of lipid from the bloodstream by the EC represents an important phenotypic modulation which may play a crucial role in atherogenesis and is probably the major pathway for lipid transport under these conditions. However, other forms of lipid handling might exist which could play supporting or competing roles.

Recent studies by Aulinskas and colleagues (2, 3) have demonstrated a short circuit pathway of lipid retro-endocytosis for low-density lipoprotein (LDL) in

fibroblasts and smooth muscle cells in vitro. After the cells were loaded with LDL, monensin or chloroquine was used to raise the intracellular pH and inhibit lysosomal acid hydrolysis, and lipid was detected re-entering the fluid medium. The structural correlates for this pathway have apparently not been identified. We present morphological evidence, obtained using conventional TEM and high-resolution SEM, suggestive of lipid retro-endocytosis by porcine coronary arterial EC during experimental atherosclerosis.

## Materials and Methods

### Animals

Four mature female Hanford miniature swine weighing 60 to 80 kg (Charles River Laboratories) were used in this study. All experimentation, animal handling, and animal care was performed according to guidelines established by the National Institutes of Health for the care and use of laboratory animals, and furthermore was conducted in such a manner as to minimize pain, stress, and discomfort to the animals.

Two swine were fed a diet of standard laboratory swine chow (controls). The other two were fed a diet of standard chow supplemented with, by weight, 2% cholesterol, 15% peanut oil, and 1.5% sodium cholate. One month after initiation of the diets, all animals underwent balloon catheter de-endothelialization injury of a proximal segment of the left anterior descending or left anterior descending or left circumflex coronary artery under inhalant anesthesia, via a femoral arteriotomy using fluoroscopic catheter guidance. The same arterial segment was re-injured 4 months later by placement of an intravascular stent prosthesis as described previously (8). One month after this secondary arterial trauma, the animals were euthanatized by anesthetic overdose and the coronary arteries were prepared as described below.

### Specimen Fixation, Preparation, and Imaging

The heart was rapidly excised after sacrifice and the left main coronary artery ostium was cannulated with large bore polyethylene tubing. The vasculature was perfused for 1-2 minutes with oxygenated 0.1 M cacodylate in 4% sucrose, pH 7.4, at 37°C and approximately 110 mm Hg pressure. Heparin (1 unit/ml) was added to prevent post mortem thrombosis, and lidocaine (0.02 mg/ml) was included to achieve a state of vasodilation. Immediately after this brief rinse perfusion, the vasculature was perfusion fixed for 10-15 minutes with oxygenated 2.5% glutaraldehyde in 0.1 M cacodylate, pH 7.4, at 37°C and approximately 110 mm Hg pressure. The cannula was then removed and the heart immersed overnight in the same fixative. Two arterial segments from each heart were excised from the epicardium, including the injured segment and a native (uninjured) segment from a separate branch of the left coronary circulation. The segments were placed in chilled 0.1 M cacodylate and trimmed of excess tissue. The injured segments were carefully cut longitudinally and transversely with scissors and razor to approximately 2 x 3 mm dimensions. The native arteries were sectioned transversely into 3 mm rings. These specimens were postfixed for one hour in 1% osmium tetroxide (in 0.1 M cacodylate) and washed briefly in distilled water. The specimens were then dehydrated through graded ethanol series to 100%.

For SEM, one specimen each of native and injured artery from both fat-fed and normal swine (4 total) were critical point dried from liquid carbon dioxide using thermoregulation and flow monitoring. They were mounted on aluminum stubs with the luminal surfaces oriented upwards and sputter coated with an ultrathin (2 nm) continuous fine grain film of chromium (Denton Instruments). In-the-lens imaging was performed at 10 and 25 kV accelerating voltage, in the SE-1 signal mode, with the specimens on the upper stage of an International Scientific Instruments DS-130 scanning electron microscope equipped with a $LaB_6$ emitter. Briefly, the SE-1 signal mode is the high-resolution imaging mode in which, using an in-the-lens imaging technique and an ultrathin metal coating, only the specimen-specific SE-1 and SE-2 electrons are collected.

For TEM, one specimen each of injured and native artery from both fat-fed and normal swine (4 total) were embedded in Epon-Araldite, sectioned to 70 nm thickness, and mounted on copper grids. They were stained with lead citrate and uranyl acetate and examined on a JEOL 100-CX transmission electron microscope operating at 80 kV accelerating voltage.

## Results

Survey SEM at low magnification revealed the presence of numerous small particles on the luminal plasmalemma of the coronary artery EC from fat-fed but not normal swine (Fig. 1). The particles were found on cells which appeared otherwise normal, being elongated with the longitudinal axis parallel to the direction of blood flow and showing no evidence of injury. They seemed to be localized primarily near the cell junctions. Also observed in survey SEM were numerous flattened, stellate cells adherent to the EC by pseudopodia (Fig. 1). These cells showed highly irregular surface topography and were seen in both native and injured segments from fat-fed and normal swine.

At higher magnifications (50,000 to 200,000X), high-resolution (HR) SEM showed that the particles on the luminal plasmalemma of fat-fed swine were roughly spheroidal structures ranging in size from approximately 250 nm to 450 nm diameter (Figs. 2-4). They appeared both singly and in clusters of up to four (Fig. 2). The surfaces of the particles were not entirely smooth but showed a degree of dimpling (Fig. 3). At the highest magnifications, HRSEM suggested segmen-

tation or compartmentalization of most of the spheroids (Fig. 4). The resolution of surface domains on both the spheroids and the EC membrane was greatly enhanced by increasing the accelerating voltage from 10 kV (Fig. 2) to 25 kV (Figs. 3 and 4).

Survey TEM (Fig. 5) provided correlation of the adherent stellate cells seen by SEM (Fig. 1). The EC displayed an increase in lysosomal compartments and occasionally showed multivesicular bodies in the cytoplasm; in one instance a multivesicular body, homologous to the spheroidal structures observed at the luminal plasmalemma, was seen in the extracellular space where it was apparently trapped by an overlying cell (Fig. 5). Higher magnification TEM confirmed that the spheroids possessed a particulate nature, with subunits ranging in size from about 20 to 150 nm diameter (Figs. 6-8). The subunits were membranous vesicles and appeared in various stages of traverse of the EC luminal plasmalemma associated with cytoplasmic inclusions and extensions of the membrane (Figs. 6 and 7). Many of the vesicles displayed a finely granulated content and a bilayer structure of their membranes (Fig. 8).

## Discussion

It is possible that the vesicular structures which we have documented could represent an artefactual phenomenon. However, we do not feel this is the case for a number of reasons. First, appropriate perfusion fixation procedures including physiologic temperature, pH, and oxygenation considerations were applied to minimize distortion during this phase of specimen preparation. Second, delicate specimen handling techniques during critical point drying were employed (thermoregulation and flow monitoring) for SEM imaging. Third, there was excellent preservation of other ultrastructural features including membranes, junctions, plasmalemmal and cytoplasmic vesicles, micropodia, and endoplasmic reticulum. Finally, there was good correlation between the SEM and TEM images of these pertinent structures. Therefore, it seems likely that these apparent lipid vesicular structures were present at and near the luminal surface of the EC, in a form similar to that which we have documented, at the time of perfusion fixation. Whether they formed rapidly (in about two minutes) between the time the animals were sacrificed and the time of arterial cannulation remains an unanswered question. This problem could be addressed by rapid freezing of the tissue in liquid nitrogen. However, since we consistently observed the lipid structures in specimens from fat-fed animals but not control specimens, with localization at EC junctions near areas of arterial branching, it seems that this was not the case.

Using certain morphological techniques only, we could not determine the precise composition or direction, if any, of transport of the structures we documented. It is possible that the observed phenomenon represents EC phagocytosis of large circulating lipid aggregates. Ryan has demonstrated the capacity of EC in culture to phagocytose unopsonized polystyrene microspheres, heat-killed *Staphylococcus aureus* bacteria, and cholesterol crystals in a time-dependent manner (9). Since we did not perform analysis of blood lipids in the swine we do not know if particles in the size range of the EC-associated structures (250-450 nm) were present in the circulation. Certainly chylomicrons are within this range and it is possible they are removed from the circulating blood by the EC of coronary arteries during hyperlipidemia. However, the appearance of the lipid vesicular structures in various apparent stages of traverse of the EC membrane is more suggestive of exocytosis (Figs. 8 and 9) than phagocytosis.

With regard to composition, the standard TEM preparation techniques used in this study did not allow differentiation between lipid droplets and vesicles, since all lipid prepared in this manner appears vesicular. Bocan et al. (4) showed that with the osmium-thiocarbohydrazide-osmium staining technique, lipid droplets and vesicles were well differentiated in human atherosclerotic plaques.

Aulinskas et al. described the retro-endocytosis pathway for low-density lipoprotein (LDL) cholesterol in bovine aortic smooth muscle cells (2) and human skin fibroblasts (3) *in vitro*. When the cells were loaded with labelled LDL by introduction into the culture medium, and normal mechanisms of LDL degradation were impaired by inhibition of lysosomal hydrolysis, the labelled LDL reappeared in the culture medium largely unchanged in composition. This pathway was described as a form of cellular "regurgitation" which was termed retro-endocytosis. It is possible that, in our swine model, a similar overloading occurred in the arterial EC exposed to a high circulating concentration of LDL and other lipids. The cells may have disposed of excess endocytosed lipid by transporting it back to the luminal space. Pasquinelli et al. (7) recently noted the appearance of lipid vesicles at the luminal and abluminal aspects of EC in atherosclerotic plaques from human carotid arteries and suggested the possibility of EC lipid discharge. Apkarian and L'Hernault (1) observed lipid structures similar to those described here associated with the capillary EC of the adrenal cortex in rhesus monkeys.

In summary, we have documented a previously unreported phenomenon in the coronary artery endothelium of atherosclerotic miniature swine using high-resolution SEM and conventional TEM. The phenomenon may represent a means of lipid exchange between the endothelium and the circulating blood. Although the composition and direction of transport of the structures described cannot be ascertained due to the static limitations of these morphologic techniques, this preliminary evidence is suggestive of EC retro-endocytosis.


**Figure 1.** Native coronary artery, fat-fed swine. Survey SEM shows numerous small particles on the EC luminal surface (arrowheads). Stellate flattened cell (*) with irregular topography is adherent to the endothelium by pseudopodia (PS). Bar = 5 $\mu$m.

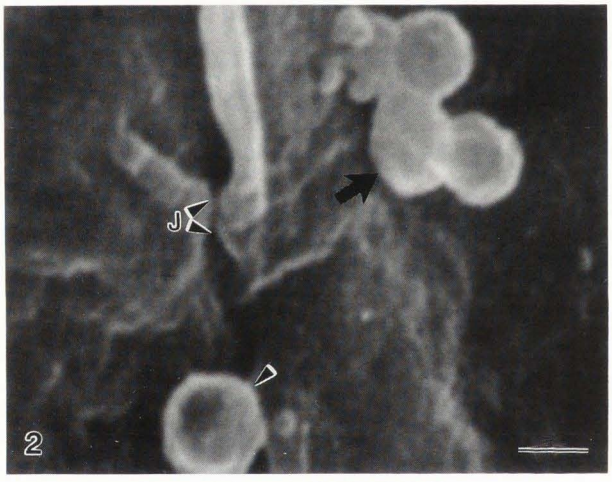


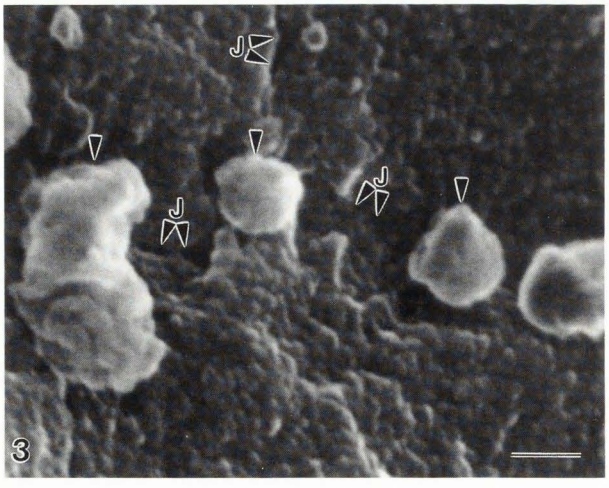


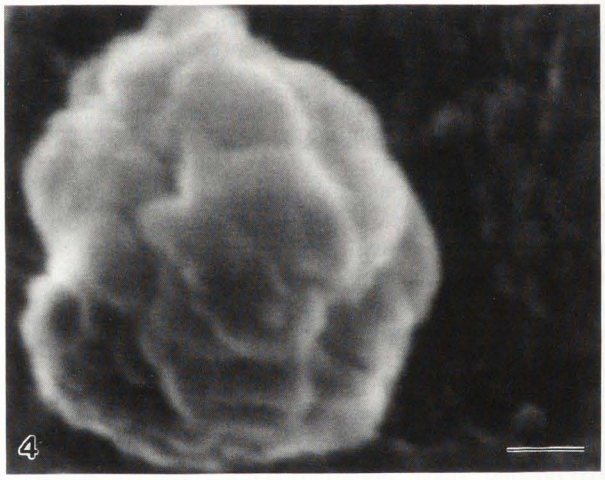


**Figure 2.** Injured coronary artery, fat-fed swine. Higher-magnification SEM shows spheroidal shape of particles which appear singly and in a cluster (arrows) near a cell junction (J). Bar = 200 nm.

**Figure 3.** Native coronary artery, fat-fed swine. Several adherent structures (arrowheads) are seen, with greatly enhanced resolution due to increased accelerating voltage (25 kV), at cell junctions (J). Bar = 100 nm.

**Figure 4.** Native coronary artery, fat-fed swine. High-resolution SEM image of spheroidal particle and EC surface. Note compartmented appearance of particle and globular EC domains. Bar = 50 nm.

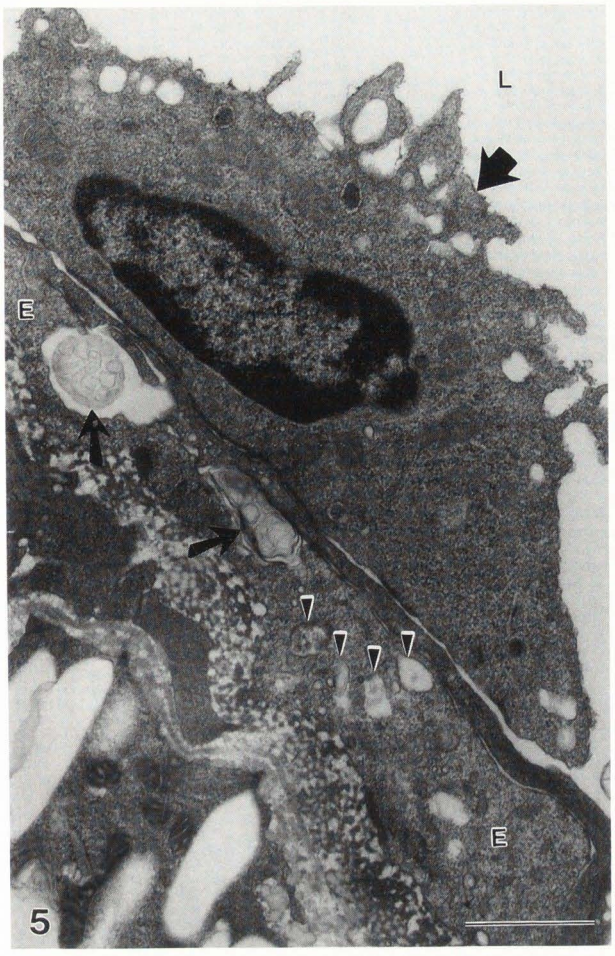


**Figure 5.** Native coronary artery, fat-fed swine. Survey TEM shows a mononuclear cell (large arrow), corresponding to adherent cell shown by SEM in Fig. 1, attached to the arterial endothelium (E). Lysosomes and multivesicular bodies (arrowheads) are seen within the EC cytoplasm, and two large multivesicular and multilamellar bodies (smaller arrows) are present in the extracellular space. L = arterial lumen. Bar = 1 $\mu$m.

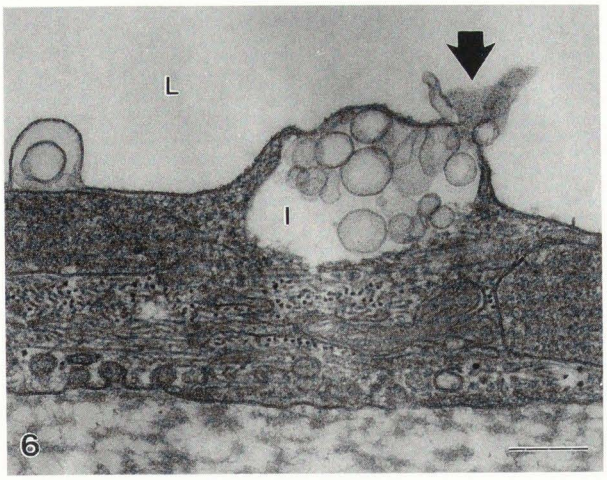


**Figure 6.** Injured coronary artery, fat-fed swine. A cytoplasmic inclusion (I) containing numerous vesicles appears to release a portion of its contents (arrow) into the arterial lumen (L). Bar = 200 nm.

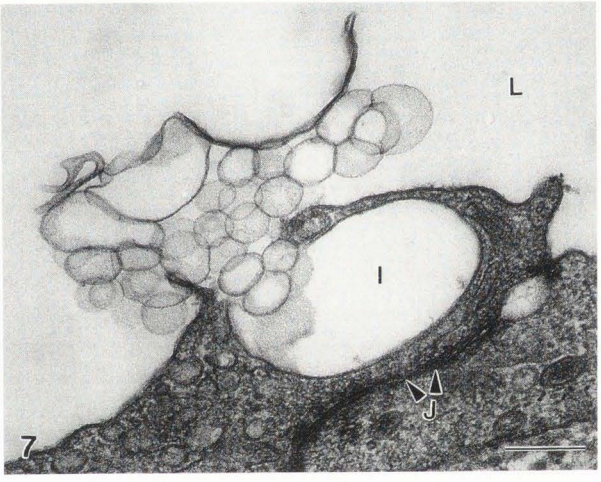


**Figure 7.** Native coronary artery, fat-fed swine. Adjacent to an EC junction (J), a cytoplasmic inclusion (I) appears to have released most of its vesicular contents into the luminal space (L). Bar = 200 nm.

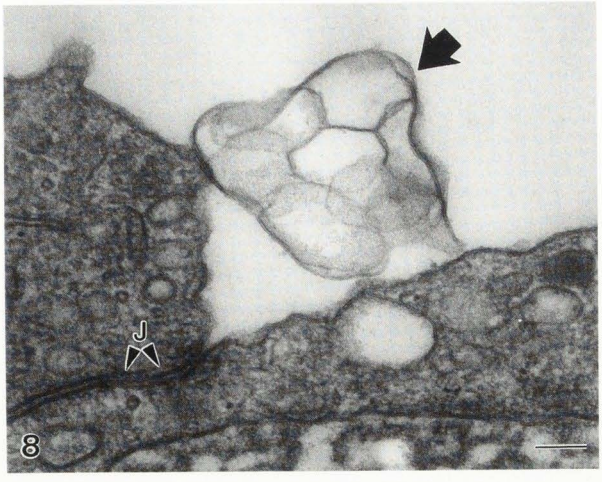


**Figure 8.** Native coronary artery, fat-fed swine. A roughly spheroidal particle (arrow), adherent to the EC surface at a cell junction (J), displays multiple vesicular subunits, most of which possess granulated content and bilayered limiting membranes. Bar = 100 nm.

**Acknowledgements**

We would like to thank Ms. Nancy L'Hernault for excellent technical assistance with TEM studies, and Mr. Nathan Karszes for skillful photographic preparation. This study was performed while KAR was a Research Associate at the Andreas Gruentzig Cardiovascular Center, Division of Cardiology, Department of Medicine, Emory University School of Medicine, and acknowledgement is given to the Center's director, Spencer King III, M.D., for his important contributions. This work was also supported in part by the National Institutes of Health Grant RR-00165 from the Division of Research Resources to the Yerkes Regional Primate Research Center.

**References**

1. Apkarian RP, L'Hernault NL (1990). Correlative light, transmission, and high-resolution (SE-1) scanning electron microscopy studies of rhesus adrenocortical morphology. Scanning Microsc. 4:125-133.

2. Aulinskas TH, van der Westhuyzen DR, Bierman EL, Gevers W, Coetzee GA (1981). Retro-endocytosis of low density lipoproteins by cultured bovine aortic smooth muscle cells. Biochim Biophys Acta 664:255-265.

3. Aulinskas TH, Oram JF, Bierman EL, Coetzee GA, Gevers W, van der Westhuyzen DR (1985). Retro-endocytosis of low density lipoprotein by cultured human skin fibroblasts. Arteriosclerosis 5:45-54.

4. Bocan TMA, Schifani TA, Guyton JR (1986). Ultrastructure of the human aortic fibrolipid lesion: formation of the atherosclerotic lipid-rich core. Am. J. Pathol. 123:413-424.

5. Fujino M (1983). Ultrastructural studies of the mouse aorta and its endothelial pinocytosis in diet-induced atherosclerosis. Acta Pathol. Jpn. 33:1115-1130.

6. Ingerman-Wojinski CM, Sedar AW, Nissenbaum M, Silver MJ, Klurfeld DM, Kritchevsky D (1983). Early morphological changes in the endothelium of a peripheral artery of rabbit fed an atherogenic diet. Exp. Mol. Pathol. 38:48-60.

7. Pasquinelli G, Cavazza A, Preda P, Stella A, Cifiello BI, Gargiulo M, D'Addato M, Laschi R (1989). Endothelial injury in human atherosclerosis. Scanning Microsc. 3:971-982.

8. Robinson KA, Roubin GS, King SB, Siegel RJ, Rodgers GP, Apkarian RP (1989). Correlated microscopic observations of arterial responses to intravascular stenting. Scanning Microsc. 3:665-679.

9. Ryan US (1988). Phagocytic properties of endothelial cells. In: Endothelial Cells (Volume III), Ryan US (Ed.), CRC Press, Boca Raton, pp 33-49.

10. Simionescu N, Vasile E, Lupu F, Popescu G, Simionescu M (1986). Prelesional events in atherogenesis: accumulation of extracellular cholesterol-rich liposomes in the arterial intima and cardiac valves of the hyperlipidemic rabbit. Am. J. Pathol. 123:109-125.

11. Trillo A, Prichard RW (1979). Early endothelial changes in experimental atherosclerosis. Lab. Invest. 41:294-302.

12. Vasile E, Antohe F, Simionescu M, Simionescu N (1989). Transport pathways of $\beta$-VLDL by aortic and normal hypercholesterolemic rabbits. Atherosclerosis 75:195-210.

13. Vasile E, Simionescu M, Simionescu N (1983). Visualization of the binding, endocytosis, and transcytosis of low-density lipoprotein by the arterial endothelium in situ. J. Cell Biol. 96:1677-1689.

**Discussion with Reviewers**

**U. Sigwart**: 0.1 M cacodylate with 4% sucrose is not the best thing to start a perfusion with (cytotoxicity). 0.1 M cacodylate used for preparation of glutaraldehyde fixation is hypertonic, as can also be seen from the condensed (dense) aspect of the cytoplasm in TEM micrographs.

**Authors**: 0.1 M cacodylate with 4% sucrose has an osmolarity of approximately 320 mOsm; 2.5% glutaraldehyde in 0.1 M cacodylate has an osmolarity of about 480 mOsm. Both of these solutions are well within the limits of standard recommendations for the osmolarity of prefixative and fixative solutions used in the preparation of vascular tissue for electron microscopy (Hayat MA, Principles and Techniques of Electron Microscopy (3rd edition), CRC Press, Boca Raton, 1990, p. 11). The 'condensed' appearance of the cytoplasm may be due to relatively heavy staining of the sections with uranium and lead salts.

**U. Sigwart**: Lipid vesicles usually have some finely granulated content. What the authors show in their procedures are membrane-bound (limited) vesicles with no content, such as in multivesicular bodies (lysosomes). 'Roughly spheroidal structures' are also seen in normal embryonic/fetal endocardium.

**Authors**: Our TEM micrographs do show vesicles with some finely granulated content (Figs. 6-8). Apkarian and L'Hernault (1), among others, have observed similar spheroidal structures associated with the capillary endothelium of the adrenal cortex, a tissue highly active in the uptake of lipoprotein and release of steroid hormones. We are very much interested in the findings regarding the existence of spheroidal structures, similar to those we observed, in embryonic and fetal endocardium.

**G. Pasquinelli**: What criteria did you use to distinguish the monocyte-derived foam cells from the smooth muscle cell-derived ones, and which subtype of foam cells was more common in these arteries?

**Authors**: Monocyte-derived foam cells were distinguished by absence of a basement membrane and cyto-

plasmic microfilaments (particularly dense bodies), and low content of pinocytotic vesicles. Although the small sample size precluded definitive assessment of the distribution of these cell subtypes, our general impression was that the smooth muscle cell-derived foam cells were more abundant in the injured coronary arteries, whereas the macrophage-foam cells predominated in the native arteries (fat-fed swine only).

**G. Pasquinelli**: Did you see subendothelial lipid vesicles at the same site where you had evidence of lipid retro-endocytosis?

**M. Richardson**: Did the intima associated with the endothelial cells showing these changes, contain lipid? If not, how close was any area of lipid deposition to these cells? If these cells are not associated with lipid deposition does this affect the interpretation that they are associated with lipid transport?

**Authors**: Again, our limited number of observations did not allow us to determine either association or dissociation of subendothelial lipid deposition with apparent retro-endocytosis. However, we did not observe in any of the TEMs the luminally positioned spheroid structures on endothelial cells which also showed substantial abluminal accumulation of lipid. Further study is needed to investigate whether there might be a relationship between these two phenomena. It is not unreasonable to speculate that in some instances, lipid retro-endocytosis may represent a defense mechanism against arterial wall cholesterol deposition. Alternatively, if retro-endocytosed cholesterol is modified, it would be chemotactic for monocytes, promoting adhesion and committing these cells towards foam cell formation.

Although transcellular carriage and luminally-directed reverse carriage may be divergent endothelial responses to lipid overload, they can both be considered forms of EC lipid transport.

**R.M. Albrecht**: Are 'retro-endocytosis' and phagocytosis as discussed mutually exclusive or could elements of phagocytosis be involved in the retro-endocytic process?

**Authors**: A strict interpretation of 'retro-endocytosis' might include that it involve cellular regurgitation only from vesicles and endosomes, since the 'short-circuit' nature of the pathway should presumably stop transport short of the lysosomal compartments. However, our TEM observations suggest a discharge from the larger end-stage degradation compartments, lysosomes and multivesicular bodies. It certainly seems possible that the material undergoing reverse carriage into the arterial lumen could have initially been taken into the cell by either 1) receptor-dependent or -independent uptake via coated pits or plasmalemmal vesicles, or 2) phagocytosis.